nature structural & molecular biology

# Asparagine endopeptidase cleaves α-synuclein and mediates pathologic activities in Parkinson's disease

Zhentao Zhang[1,2], Seong Su Kang[2], Xia Liu[2], Eun Hee Ahn[2], Zhaohui Zhang[1], Li He[3], P Michael Iuvone[3,4], Duc M Duong[5,6], Nicholas T Seyfried[5,6], Matthew J Benskey[7], Fredric P Manfredsson[7], Lingjing Jin[8], Yi E Sun[8], Jian-Zhi Wang[9] & Keqiang Ye[2]

**Aggregated forms of α-synuclein play a crucial role in the pathogenesis of synucleinopathies such as Parkinson's disease (PD). However, the molecular mechanisms underlying the pathogenic effects of α-synuclein are not completely understood. Here we show that asparagine endopeptidase (AEP) cleaves human α-synuclein, triggers its aggregation and escalates its neurotoxicity, thus leading to dopaminergic neuronal loss and motor impairments in a mouse model. AEP is activated and cleaves human α-synuclein at N103 in an age-dependent manner. AEP is highly activated in human brains with PD, and it fragments α-synuclein, which is found aggregated in Lewy bodies. Overexpression of the AEP-cleaved α-synuclein$_{1–103}$ fragment in the substantia nigra induces both dopaminergic neuronal loss and movement defects in mice. In contrast, inhibition of AEP-mediated cleavage of α-synuclein (wild type and A53T mutant) diminishes α-synuclein's pathologic effects. Together, these findings support AEP's role as a key mediator of α-synuclein-related etiopathological effects in PD.**

PD is characterized by the degeneration of dopaminergic neurons in the substantia nigra (SN) pars compacta. The etiology of PD appears to be multifactorial, involving both genetic and environmental components. To date, several cellular mechanisms, such as aberrant protein folding, oxidative stress and mitochondrial dysfunction have been implicated in the development and progression of this disease[1]. Most PD cases are sporadic, and their pathogenesis is unclear. However, several cases of familial PD have been described in which mutant genes have been identified as being causative in this disorder. These genes include the abundant presynaptic protein α-synuclein[2,3] and two components of the proteasome pathway: L1 ubiquitin C-terminal hydrolase[4] and parkin[5]. The misfolding of α-synuclein, the main component of Lewy pathology, plays a key role in the etiopathogenesis of PD, because the disorder is characterized by the accumulation of intraneuronal protein aggregates (Lewy bodies and Lewy neurites)[6]. Several mutations in the gene encoding α-synuclein, including A30P, A53T and E64K, have been identified in dominant forms of familial PD[2,3]. Moreover, duplication or triplication of the wild-type α-synuclein-encoding gene also causes PD, thus indicating that an increased α-synuclein protein level is sufficient to cause the disease. Furthermore, single-nucleotide polymorphisms in the α-synuclein-encoding gene are associated with an increased risk of developing sporadic PD[7]. The potential mechanisms of α-synuclein in PD have been explored by transgenic expression of human α-synuclein in various models[8–10]. Although these studies have demonstrated a pathological effect resulting from transgenic expression, including the formation of inclusion bodies, the molecular mechanisms involved in neurodegeneration remain obscure.

The physiological function of α-synuclein is poorly understood[11]. α-Synuclein is widely expressed in the nervous system, where it is found in presynaptic nerve terminals, closely associated with presynaptic vesicles[11]. The neurotoxicity of α-synuclein may be related to its oligomerization and fibrillization[12] or may be due to a loss of functional protein, owing to the formation of insoluble aggregates. Mounting evidence indicates that C-terminal truncation promotes α-synuclein fibrillization[13–16], in a process mediated by numerous proteases such as calpain[17,18] and cathepsin D[19,20]. However, whether these proteases proteolytically cleave α-synuclein and mediate their pathological effects in an age-dependent manner in PD etiopathology remains unclear.

Mammalian AEP (also called legumain) is an endolysosomal cysteine protease that cleaves proteins after asparagine residues. AEP is synthesized as an inactive zymogen, and its activation requires sequential removal of C- and N-terminal propeptides at different pH

[1]Department of Neurology, Renmin Hospital of Wuhan University, Wuhan, China. [2]Department of Pathology and Laboratory Medicine, Emory University School of Medicine, Atlanta, Georgia, USA. [3]Department of Ophthalmology, Emory University School of Medicine, Atlanta, Georgia, USA. [4]Department of Pharmacology, Emory University School of Medicine, Atlanta, Georgia, USA. [5]Department of Biochemistry, Emory University School of Medicine, Atlanta, Georgia, USA. [6]Center for Neurodegenerative Diseases, Emory University School of Medicine, Atlanta, Georgia, USA. [7]Translational Science and Molecular Medicine, Michigan State University, College of Human Medicine, and Hauenstein Neuroscience Center, Mercy Health Saint Mary's, Grand Rapids, Michigan, USA. [8]Translational Center for Stem Cell Research, Tongji Hospital, Department of Regenerative Medicine, Tongji University School of Medicine, Shanghai, China. [9]Pathophysiology Department, School of Basic Medicine and the Collaborative Innovation Center for Brain Science, Key Laboratory of the Ministry of Education of China for Neurological Disorders, Tongji Medical College, Huazhong University of Science and Technology, Wuhan, China. Correspondence should be addressed to K.Y. (kye@emory.edu), L.J. (lingjingjin@163.com) or J.-Z.W. (wangjz@mails.tjmu.edu.cn).

Received 22 December 2016; accepted 14 June 2017; published online 3 July 2017; doi:10.1038/nsmb.3433

thresholds[21,22]. AEP activity is controlled by the cysteine protease inhibitor cystatin C[23]. Recently, we have reported that neuronal AEP is activated by acidosis during excitotoxicity and contributes to neuronal apoptosis by degrading the DNase inhibitor SET[24,25]. Moreover, AEP-generated SET fragments inhibit protein phosphatase-2A and enhance tau hyperphosphorylation[26]. We have also shown that AEP cleaves TAR DNA-binding protein 43 in brain samples from humans with frontotemporal lobar degeneration[27]. Most recently, we have found that AEP cleaves tau at residues N255 and N368, thereby mediating formation of neurofibrillary tangles in human brains with Alzheimer's disease (AD)[28]. Further, we have found that AEP acts as a δ-secretase that cleaves APP at residues N373 and N585, thereby regulating BACE1 fragmentation of the C-terminal fragment of APP and resulting in β-amyloid generation. Deletion of AEP from tau P301S or 5XFAD transgenic mice substantially alleviates the pathological and cognitive defects[28,29].

PD is a chronic neurodegenerative disease, and aging is the major risk factor for PD development. We have recently reported that AEP protein levels are increased in the brain in an age-dependent manner[28,29]. Hence, it is possible that AEP might also process α-synuclein in the brains of people with PD during aging. In the current study, we tested this hypothesis and found that AEP cleaves α-synuclein at N103 in the human PD brain and promotes α-synuclein aggregation and neurotoxicity. Interestingly, AEP is activated in an age-dependent manner and contributes to and/or is concurrent with α-synuclein truncation in the SN. Overexpression of the α-synuclein$_{1-103}$ fragment in the rodent SN induces dopaminergic neurodegeneration and a resultant motor phenotype, whereas blockade of cleavage of α-synuclein (either wild type or A53T mutant) by AEP ameliorates these α-synuclein-mediated pathological effects. Hence, our observations demonstrate that AEP contributes to the α-synuclein pathogenic activity in PD.

## RESULTS

### Cleavage of α-synuclein at N103 in PD and Lewy body dementia

To investigate the proteolytic processing of α-synuclein in PD, we conducted a proteomic analysis with immunoprecipitated α-synuclein from PD brains. Notably, LC–MS/MS analysis revealed an α-synuclein peptide fragment cleaved at N103 from the partial tryptic peptides (**Fig. 1a**). To detect the α-synuclein N103 fragment, we generated a neoepitope antibody (designated anti-N103) that specifically recognized the cleaved α-synuclein N103 fragment but not the full-length protein. ELISA measurements demonstrated that this antibody was highly selective for the α-synuclein$_{1-103}$ fragment rather than intact α-synuclein (**Supplementary Fig. 1a**). Western blot analysis with recombinant full-length (FL) α-synuclein and its fragment comprising residues 1–103 confirmed that this antibody selectively recognized α-synuclein$_{1-103}$ but not FL α-synuclein. The antibody also immunoprecipitated the cleaved N103 fragment from PD brains (**Fig. 1b**,**c**). To confirm that α-synuclein cleavage after N103 indeed occurs in people with synucleinopathy, we conducted immunohistochemistry (IHC) assays. IHC analysis of brain sections with anti–α-synuclein N103 clearly indicated that α-synuclein was cleaved after N103 in brains with PD or Lewy body dementia (LBD) but not in control brains without synucleinopathy. The antibody specificity was corroborated with a blocking peptide (**Fig. 1d**). Immunofluorescence (IF) staining confirmed that the α-synuclein N103 fragment was present as aggregates in Lewy bodies and synaptic structures (**Fig. 1e** and **Supplementary Fig. 1b**). Immunoblotting with the α-synuclein N103–specific antibody revealed that α-synuclein N103 was elevated specifically in both the soluble and insoluble fractions of SN tissues from PD brains, and its level was much higher than that observed in cortical tissues from the same subjects. By contrast, α-synuclein N103 was scarcely detectable in both brain regions in controls without synucleinopathy (**Fig. 1f**). Remarkably, α-synuclein N103 was readily detectable in brains with LBD compared with controls. These findings were further confirmed with anti-α-synuclein antibody. Interestingly, AEP was activated in the LBD brain samples, and this activation correlated with α-synuclein fragmentation patterns (**Fig. 1g** and **Supplementary Fig. 1c–e**). Thus, α-synuclein N103 fragmentation occurred predominantly in brains with PD or LBD but not in controls without synucleinopathy.

### AEP cuts human α-synuclein at residue N103

AEP is the only reported mammalian enzyme that cleaves C terminal to asparagine. Hence, we hypothesized that AEP is responsible for the cleavage of α-synuclein after N103. To test this hypothesis, we transfected N-terminally GFP-tagged human α-synuclein into HEK293 cells and incubated cell lysates with kidney lysates (pH 7.4 or 6.0) prepared from wild-type or AEP-knockout mice. A truncated α-synuclein band was selectively observed in wild-type kidney lysates at pH 6.0 but was not observed in AEP-knockout kidney lysates or at pH 7.4. The cleavage of α-synuclein was reconstituted when exogenous active AEP was added to the AEP-knockout reactions (**Fig. 2a**). AEP enzymatic activity in the reactions was confirmed (**Fig. 2a**). GFP-tagged α-synuclein was also cleaved in mouse brain lysates in the same pattern as that in kidney lysates (**Fig. 2b**). We also tested the cleavage of C-terminally GFP-tagged α-synuclein in mouse kidney and brain lysates, and found the same results (**Fig. 2c**,**d**). When GFP-α-synuclein was incubated with wild-type kidney lysates for 5, 10 or 15 min, the intensity of the truncated α-synuclein fragment increased over time at pH 6.0 (**Fig. 2e**), thus indicating that AEP in the active kidney lysates truncates α-synuclein in a time-dependent manner. Cys189 is essential for the protease activity of AEP, and cleavage after N323 is obligatory for the maturation of the protease[30]. As expected, α-synuclein was cleaved by wild-type but not by mutated (C189S or N323A) AEP, thereby indicating that AEP's enzymatic activity was responsible for the observed α-synuclein proteolytic cleavage (**Fig. 2f**). AEP is selectively inhibited by the small peptide AENK but not the control peptide AEQK[24]. Accordingly, AENK but not AEQK selectively antagonized GFP-α-synuclein cleavage by active AEP in a dose-dependent manner (**Fig. 2g**). Furthermore, recombinant active AEP directly cleaved recombinant α-synuclein in a time-dependent manner, and the resultant fragment was recognized by anti–α-synuclein N103 antibody. The cleavage was blocked by the AEP inhibitor AENK (**Fig. 2h**,**i**). Together, these results indicated that α-synuclein is a direct biological substrate of AEP.

To determine whether there are multiple AEP-cleavage sites in α-synuclein, we conducted a mapping assay with a variety of truncated α-synuclein recombinant proteins. FL α-synuclein produced a fragment of the same size as the 1–103 fragment, thus indicating that α-synuclein was cut near residue 103 (**Supplementary Fig. 2a**). MS analysis identified the α-synuclein N103 fragment from purified mammalian GST-α-synuclein recombinant proteins cleaved by active AEP *in vitro* (**Supplementary Fig. 2b**). Because AEP selectively cleaves its substrates after asparagine residues, and human α-synuclein contains three asparagine residues (N65, N103 and N122), we prepared three α-synuclein point mutants with asparagine changed to alanine. Both N-terminal and C-terminal GFP-tagged α-synuclein N65A and N122A mutants were cleaved as efficiently as wild-type α-synuclein by AEP, whereas the N103A mutation completely abolished cleavage (**Supplementary Fig. 2c**,**d**). Interestingly, mouse

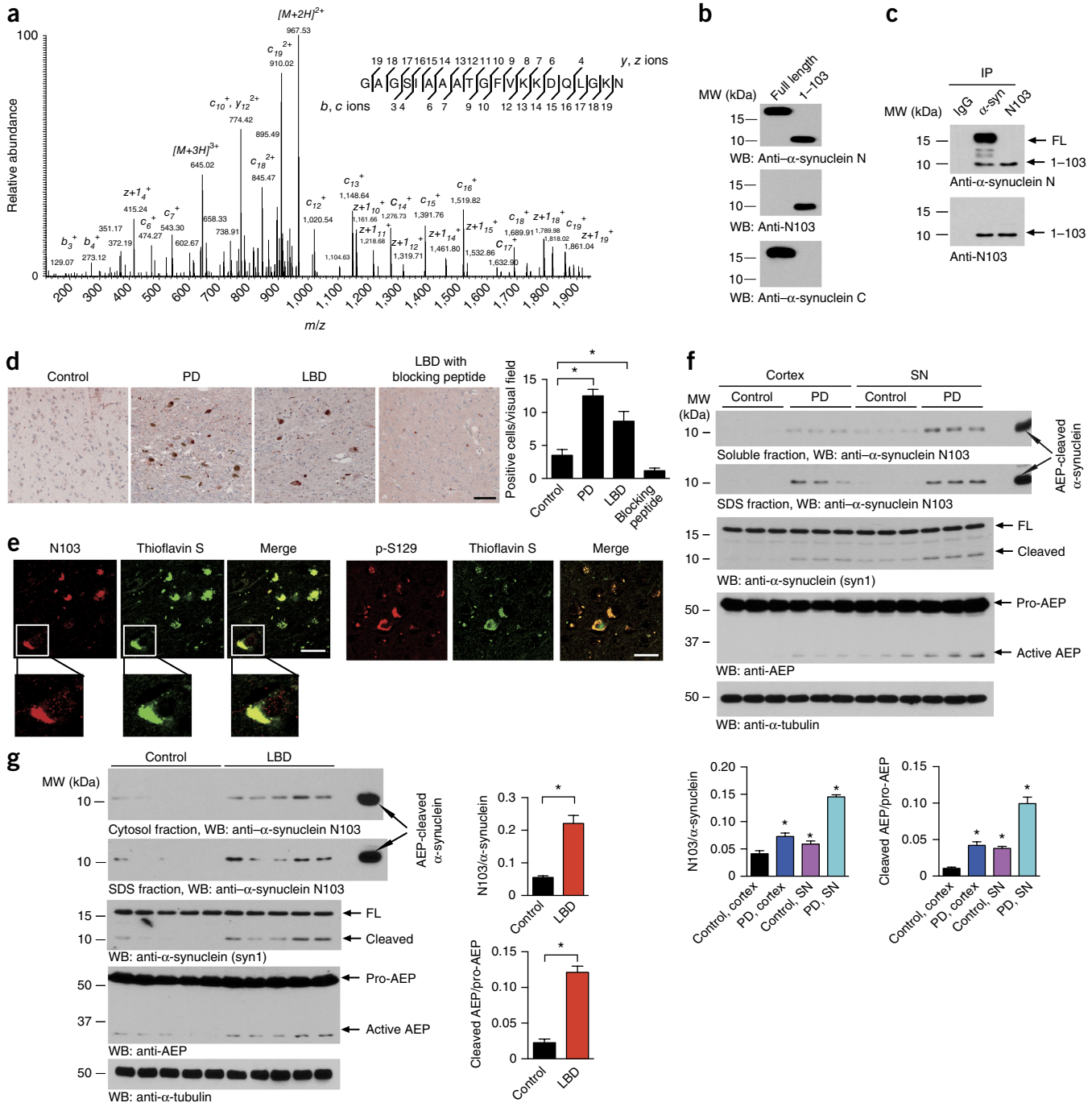


**Figure 1** α-synuclein is truncated after N103 in PD and LBD brains. (**a**) MS/MS spectrum showing the cleavage of α-synuclein after N103 in brain samples from subjects with PD. (**b**) Western blot (WB) with anti-α-synuclein antibodies. FL α-synuclein or the α-synuclein$_{1–103}$ fragment were detected by immunoblotting with anti–α-synuclein N-terminus (N) antibody, anti–α-synuclein C-terminus (C) antibody and anti–α-synuclein N103 antibody. MW, molecular weight. (**c**) Immunoprecipitation (IP) of α-synuclein (α-syn) from human PD brain lysates with anti–α-synuclein N-terminus or anti–α-synuclein N103 antibodies. (**d**) Immunohistochemistry of the α-synuclein N103 fragment in SN sections from people with PD and cortex sections from people with LBD. Scale bar, 50 μm. Bar graph, quantification of positive cells in samples. Data are mean ± s.e.m.; $n = 6$ patients; $^*P < 0.05$ by one-way ANOVA. (**e**) Brain sections were immunostained with anti–α-synuclein N103 or anti–phospho (p)-S129-α-synuclein (red) and then stained with thioflavin S (green), which stains Lewy bodies. Scale bars, 20 μm. Images are representative of nine sections from three subjects with LBD. (**f**,**g**) Western blots showing the presence of the α-synuclein N103 fragment in soluble and insoluble fractions of tissues from people with PD (**f**) or LBD (**g**), but not age-matched control tissues. α-Tubulin, loading control. Bar graphs show quantification as mean ± s.e.m.; $n = 3$ patients in **f**, $n = 5$ patients in **g**; $^*P < 0.05$ compared with control, by one-way ANOVA in **f** and two-tailed Student's $t$ test in **g**. Results for an independent cohort of samples are shown in **Supplementary Figure 1c**,**d**. Blots shown are representative of three independent experiments; uncropped images are shown in **Supplementary Data Set 1**. Source data for graphs are available online.

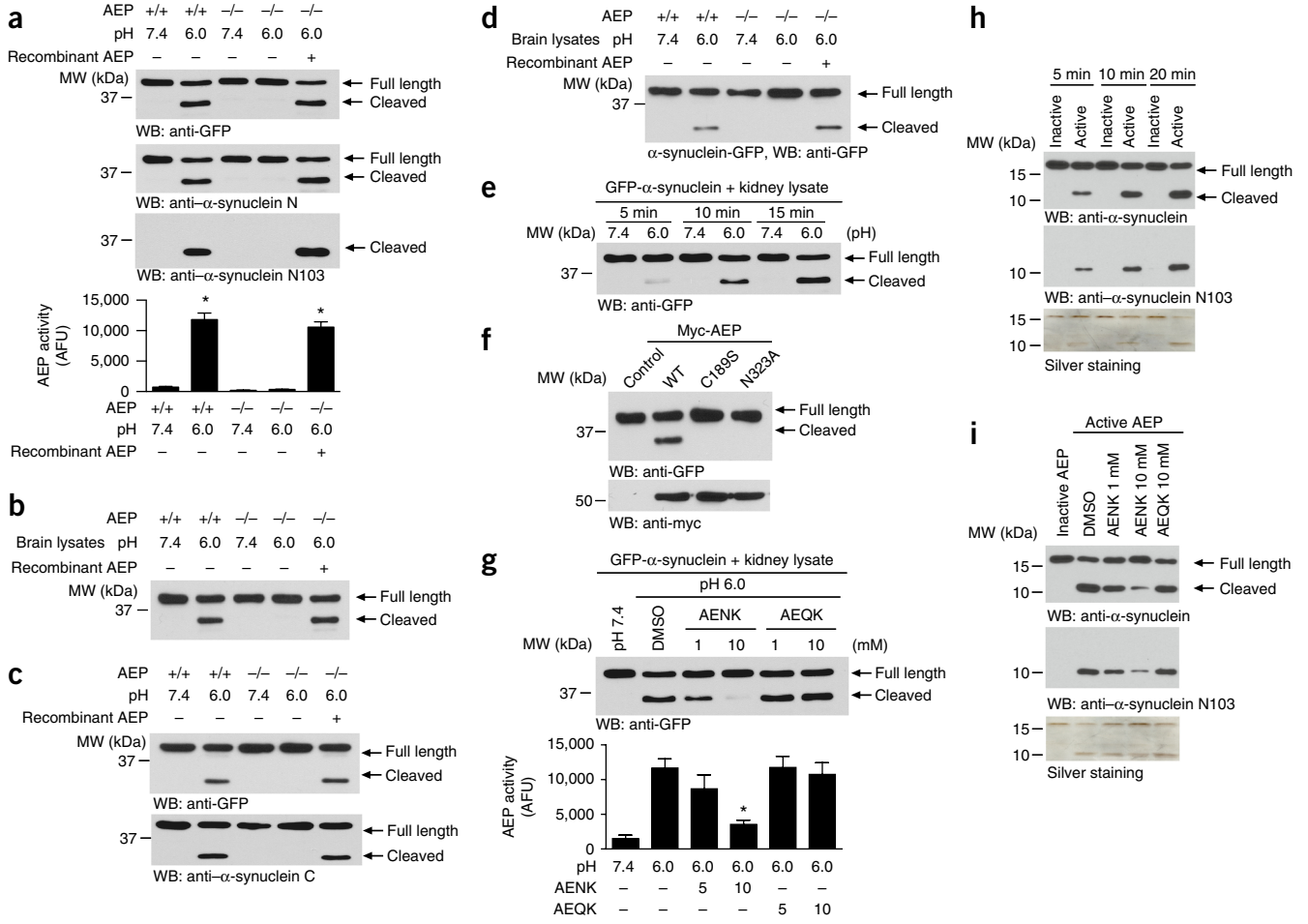


**Figure 2** α-synuclein is a substrate of AEP. (**a**) α-synuclein cleavage assay in kidney lysates. N-terminal GFP-tagged α-synuclein was incubated with kidney lysates from wild-type (+/+) or AEP-knockout (–/–) mice at pH 7.4 or pH 6.0 at 37 °C for 15 min. Western blot (WB) showing α-synuclein cleavage at pH 6.0 (top) when AEP was activated (bottom). Bar graph shows data as mean ± s.e.m.; $n = 3$ independent experiments; $^*P < 0.05$ compared with the pH 7.4 group by one-way ANOVA. AFU, arbitrary fluorescence units. (**b**) α-synuclein cleavage assay in brain lysates. N-terminally GFP-tagged α-synuclein was incubated with brain lysates from wild-type or AEP-knockout mice at pH 7.4 or pH 6.0 at 37 °C for 15 min. (**c**,**d**) Processing of C-terminally GFP-tagged α-synuclein in mouse kidney lysates (**c**) and brain lysates (**d**). (**e**) Time-dependent cleavage of α-synuclein by AEP. (**f**) α-Synuclein cleavage by wild-type and mutant AEP. (**g**) The proteolysis of α-synuclein is blocked by AENK peptide but not AEQK peptide (top). The effect of AENK on AEP was confirmed by an enzymatic activity assay (bottom). Graph shows mean ± s.e.m.; $n = 3$ independent experiments; $^*P < 0.05$ compared with wild type, by one-way ANOVA. (**h**) Recombinant AEP has high cleavage activity toward recombinant α-synuclein. The AEP-generated α-synuclein fragment was recognized by anti–α-synuclein N103 antibody. Silver-stained gel shows all the fragments. (**i**) AEP inhibitor blocks the cleavage of recombinant α-synuclein by AEP. Silver-stained gel shows all the fragments. Blots shown are representative of three independent experiments; uncropped images are shown in **Supplementary Data Set 1**. Source data for graphs are available online.



α-synuclein does not contain residue N103, but human α-synuclein does. Accordingly, human but not mouse α-synuclein was selectively fragmented by AEP (**Supplementary Fig. 2e**,**f**).

To confirm the interaction between AEP and α-synuclein, we performed coimmunoprecipitation and found that α-synuclein interacted with AEP in human PD brains (**Supplementary Fig. 3a**), where it may cleave α-synuclein. The proteolytic actions in human PD brain lysates were selectively blocked by anti-AEP but not control IgG, thus supporting the specific processing of α-synuclein N103 by AEP (**Supplementary Fig. 3b**). Immunofluorescence staining with human brain slides revealed that AEP strictly colocalized with LAMP1, the specific marker for lysosomes in control brains, whereas it leaked out into the cytoplasm and was not tightly colocalized with LAMP1 in PD brains (**Supplementary Fig. 3c**). Indeed, our subcellular fractionation assay also demonstrated that the activity of AEP was enhanced in the cytoplasm in PD brains compared with controls (**Supplementary Fig. 3d**). Cleavage assays with exogenous α-synuclein recombinant proteins demonstrated that PD and LBD brain cytosolic fractions displayed much stronger N103 cleavage activities than those of control cytosolic fractions, whereas the lysosomal fractions exhibited similar effects among control, PD and LBD brains (**Supplementary Fig. 3e**). These results suggested that AEP may leak from the lysosomes into the cytoplasm, where it cleaves α-synuclein in synucleinopathies.

## AEP cleaves α-synuclein independently of post-translational modifications

Phosphorylation of α-synuclein at S129 and Y125 regulates α-synuclein aggregation and toxicity[31]. To test whether S129 phosphorylation influences α-synuclein cleavage by AEP, we conducted an *in vitro* cleavage assay using recombinant α-synuclein and S129-phosphorylated α-synuclein. The S129-phosphorylated and nonphosphorylated α-synuclein were cleaved in a time-dependent manner with similar

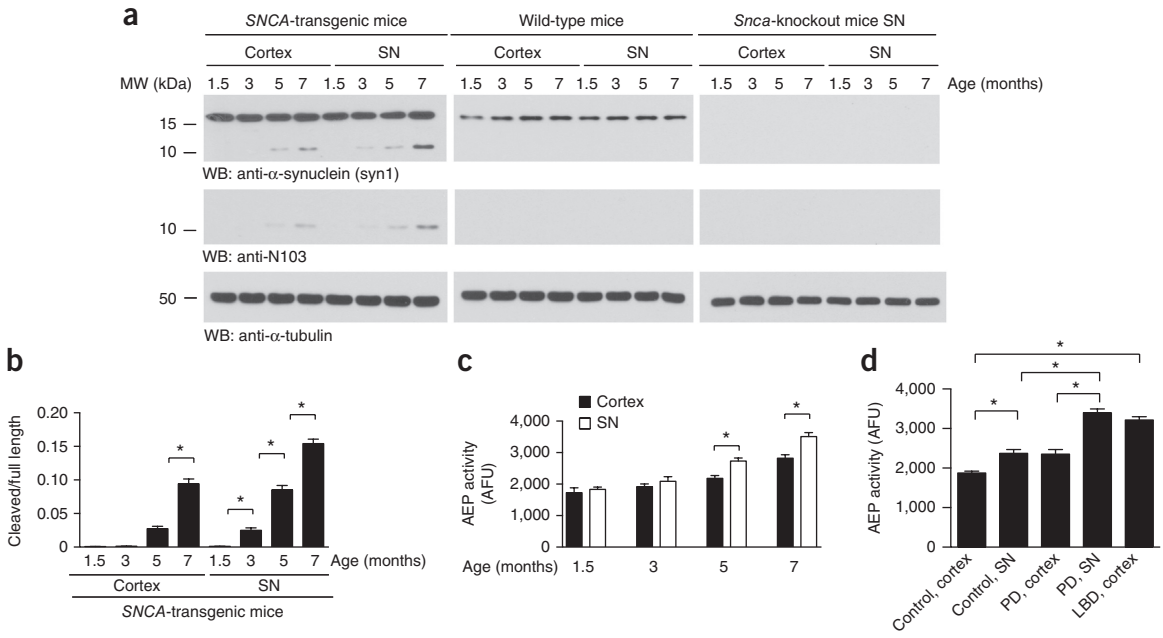


**Figure 3** AEP is activated and cleaves α-synuclein in an age-dependent manner. (**a**) Western blot (WB) showing the processing of α-synuclein during aging in human *SNCA*-transgenic mice. α-Tubulin, loading control. (**b**) Quantification of AEP-cleaved α-synuclein in the cortex and SN of *SNCA*-transgenic mice at different ages. Data are mean ± s.e.m.; $n = 3$ mice per group; $^*P < 0.05$ by one-way ANOVA. (**c**) AEP activity in the cortex and SN in *SNCA*-transgenic mice at different ages. Data are mean ± s.e.m.; $n = 5$ mice per group; $^*P < 0.05$ by one-way ANOVA. AFU, arbitrary fluorescence units. (**d**) AEP activity in the cortex and SN from PD, LBD and age-matched control tissues. Data are mean ± s.e.m.; $n = 4$ different subjects for control and LBD samples; $n = 3$ different subjects for PD samples; $^*P < 0.05$ by one-way ANOVA. Blots shown are representative of three independent experiments; uncropped images are shown in **Supplementary Data Set 1**. Source data for graphs are available online.

rates, thus indicating that phosphorylation of α-synuclein at S129 does not interfere with AEP cleavage (**Supplementary Fig. 4a**). α-Synuclein is also phosphorylated at Y125 by the Src family protein tyrosine kinase Fyn[32]. Nonetheless, both wild-type human α-synuclein and the Y125F mutant exhibited comparable cleavage rates by AEP (**Supplementary Fig. 4b**). Moreover, phosphorylation of α-synuclein at Y125 by overexpression of constitutively active or kinase-dead Fyn mutants did not affect its cleavage rate, thus further confirming that Y125 phosphorylation does not affect human α-synuclein cleavage (**Supplementary Fig. 4c**,**d**). We also tested the cleavage rate of the familial PD-associated A53T and A30P missense mutations and found that these mutants were also cleaved at the same rate as wild-type α-synuclein (**Supplementary Fig. 4e**). A number of proteinases have been implicated in α-synuclein cleavage, including calpain, cathepsin D and the proteasome[33]. To explore their potential effects on N103 fragmentation, we used specific inhibitors or a protease-inhibitor cocktail inhibiting serine proteases, aminpeptidases, cysteine proteases and acid proteases. Notably, α-synuclein cleavage was inhibited by only the peptide inhibitor AENK but not by any of the other protease inhibitors or the protease-inhibitor cocktail (**Supplementary Fig. 4f**). Thus, these results indicated that AEP is the major protease cleaving human α-synuclein at N103, and its proteolytic activity is independent of other post-translational modifications.

## AEP is activated and cleaves α-synuclein in an age-dependent manner

We have recently reported that AEP is selectively upregulated and activated in the brain in an age-dependent manner[28,29]. To explore whether this enzyme truncates human α-synuclein in a similar temporal pattern, we used a mouse transgenic model with the mouse α-synuclein-encoding gene (*Snca*) replaced with a human version, and we performed immunoblotting on SN and cortex-tissue samples from mice at 1.5, 3, 5 and 7 months of age. We found that α-synuclein was cleaved at N103 in an age-dependent manner. Fragmentation was clearly more prominent in the SN than the cortex, in a manner tightly coupled to the spatial and temporal patterns of AEP activity. In contrast, no cleavage signals were detected in wild-type or *Snca*-knockout SN tissues (**Fig. 3a–c**). Therefore, these findings indicated that AEP specifically cleaves human α-synuclein in an age-dependent manner, more prominently in the SN region than in the cortex. We also extended these studies to wild-type mice and found that AEP activity increased in an age-dependent manner, and the SN activity was much higher than that in the cortex (**Supplementary Fig. 5**). Interestingly, we observed the same result in SN and cortex samples from human PD brains (**Fig. 3d**). Hence, AEP is prone to being activated in the SN versus the cortex.

## Cleavage of α-synuclein by AEP promotes its aggregation and toxicity

To determine the effect of AEP cleavage of α-synuclein on fibrillization, we monitored the kinetics of filament formation by FL α-synuclein or the AEP-derived α-synuclein$_{1–103}$ fragment at different concentrations, by using thioflavin T staining. We found that the α-synuclein$_{1–103}$ fragment aggregated much faster and to a greater extent than did FL α-synuclein (**Fig. 4a**). Ultracentrifugation assays revealed that more aggregated α-synuclein$_{1–103}$ than FL α-synuclein was present in the pellet (**Fig. 4b**). Electron microscopy confirmed the aggregation of α-synuclein into fibrils (**Supplementary Fig. 6a**). Furthermore, the α-synuclein$_{1–103}$ fragment significantly promoted the aggregation of FL α-synuclein even at very low concentrations (**Fig. 4c**). We also tested the seeding capacity of fibrils from the α-synuclein$_{1–103}$ fragment and that from the full-length protein.

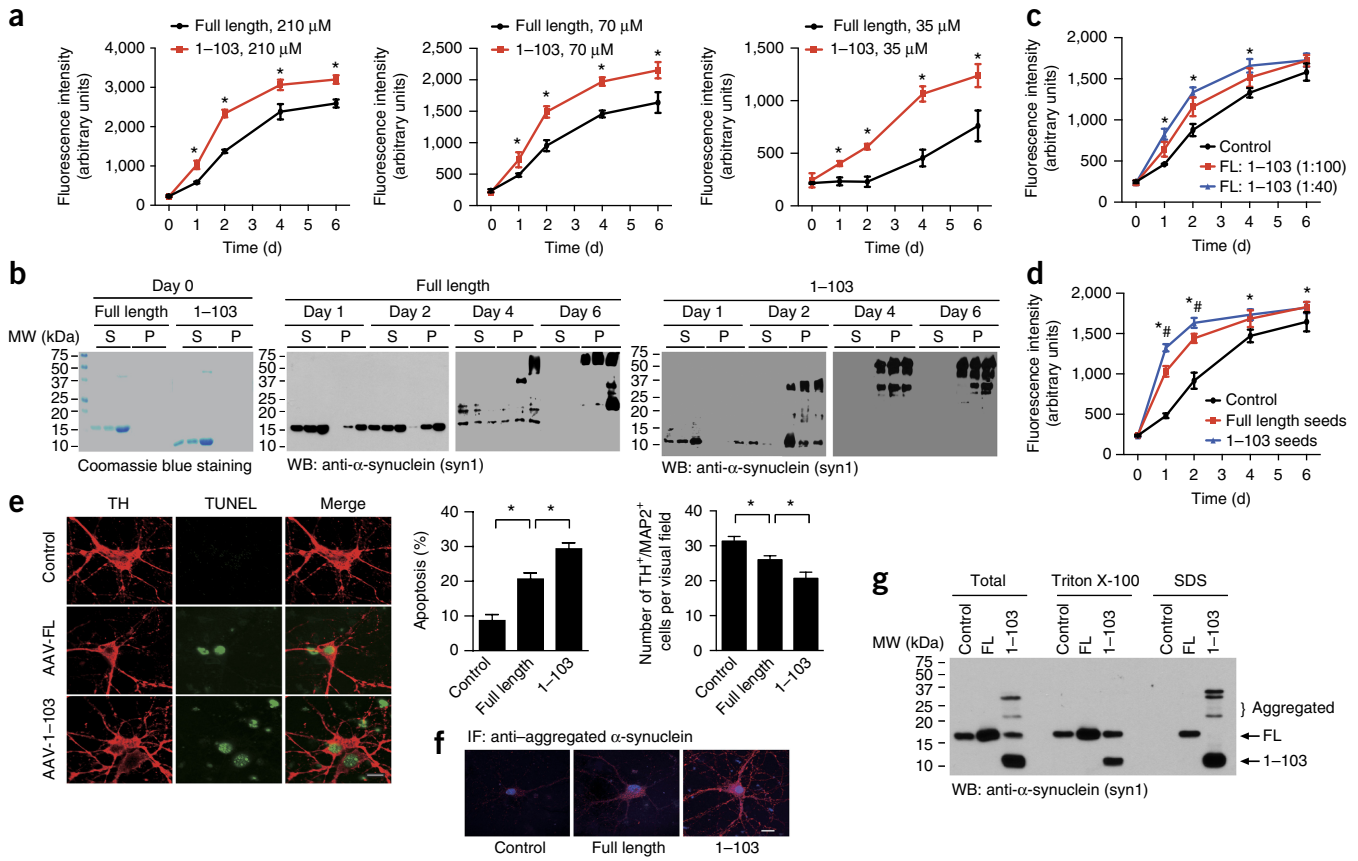


**Figure 4** AEP cleavage of α-synuclein promotes α-synuclein aggregation and toxic effects. (**a**) Thioflavin T assay showing the kinetics of aggregation of purified recombinant FL α-synuclein and the α-synuclein$_{1–103}$ fragment at different concentrations. Data are mean ± s.e.m.; $n = 3$ independent experiments; $^*P < 0.05$ by two-tailed Student's $t$ test. (**b**) Ultracentrifugation assay. The soluble and aggregated α-synuclein was analyzed by western blotting (S, supernatant; P, pellet). The blots shown are representative of three independent experiments. (**c**) The α-synuclein$_{1–103}$ fragment promotes the aggregation of FL α-synuclein. 70 μM α-synuclein aggregation was assessed with thioflavin T assays in the presence of 1:100 or 1:40 α-synuclein$_{1–103}$ fragment. Data are mean ± s.e.m.; $n = 3$ independent experiments; $^*P < 0.05$ compared with control, by one-way ANOVA. (**d**) Seeding of full-length α-synuclein by fibrils of the α-synuclein$_{1–103}$ fragment (blue) or fibrils of FL α-synuclein (red). Data are mean ± s.e.m.; $n = 3$ independent experiments; $^*P < 0.05$ compared with control; $^{\#}P < 0.05$ compared with fibrils from FL α-synuclein, by one-way ANOVA. (**e**) The neurotoxicity of FL α-synuclein and the α-synuclein$_{1–103}$ fragment. α-Synuclein (without tag) was expressed in primary cultured SN neurons. Cell death was determined by TUNEL staining and TH$^+$/MAP2$^+$ cell counts. Scale bar for micrographs, 20 μm. Data shown in graphs are mean ± s.e.m.; $n = 3$ independent experiments; $^*P < 0.05$ by one-way ANOVA. (**f**) Immunostaining showing the aggregation of α-synuclein. Scale bar, 20 μm. (**g**) Western blot (WB) showing the aggregation of α-synuclein$_{1–103}$ fragments into higher-molecular-weight species. Blots shown are representative of three independent experiments; uncropped images are shown in **Supplementary Data Set 1**. Source data for graphs are available online.

We found that α-synuclein$_{1–103}$ fibrils, compared with FL α-synuclein fibrils, seeded the α-synuclein with a much higher capacity (**Fig. 4d**). Thus, these findings suggested that AEP cleavage of α-synuclein may promote α-synuclein aggregation.

α-Synuclein truncation and oligomerization are tightly associated with its neurotoxicity[12]; therefore, we conducted dopaminergic neuronal cell death assays. As expected, overexpression of α-synuclein induced apoptosis of dopaminergic neurons, and this effect was more pronounced with the α-synuclein$_{1–103}$ fragment (**Fig. 4e**). In addition, the α-synuclein$_{1–103}$ fragment formed more aggregates, as indicated by IF staining with an antibody specific to aggregated α-synuclein (**Fig. 4f**). Furthermore, the α-synuclein$_{1–103}$ fragment formed more abundant higher-molecular-weight species than did FL α-synuclein (**Fig. 4g**). Hence, the AEP-derived α-synuclein N103 fragment is more prone to aggregation and exhibits stronger neurotoxicity. IF staining and subcellular fractionation assays indicated that most FL and truncated α-synuclein localized in the cytosolic fraction (**Supplementary Fig. 6b,c**).

### AEP-cleaved α-synuclein induces dopamine neuronal loss and motor deficits *in vivo*

To assess the pathological roles of the α-synuclein$_{1–103}$ fragment *in vivo*, we used adenoassociated viruses (AAVs) expressing either FL wild-type α-synuclein or the 1–103 fragment, which were delivered by unilateral injection into the mouse SN. Four months after the vector delivery, we performed IHC and IF staining on the brain sections to validate transduction. IHC analysis with LB509, an antibody recognizing residues 115–122 of human α-synuclein, revealed that FL α-synuclein was strongly expressed, whereas the α-synuclein$_{1–103}$ fragment was not detected (**Supplementary Fig. 7a**). By contrast, IF with the specific anti–α-synuclein N103 antibody demonstrated robust immunoreactivity toward α-synuclein$_{1–103}$ in brains injected with AAVs expressing the α-synuclein$_{1–103}$ fragment. In addition, some α-synuclein N103 signal was detectable in brains injected with FL human α-synuclein (**Supplementary Fig. 7b**), thus indicating that the FL human α-synuclein had been truncated at N103 in the SN. Immunoblotting with the same specific antibodies selectively

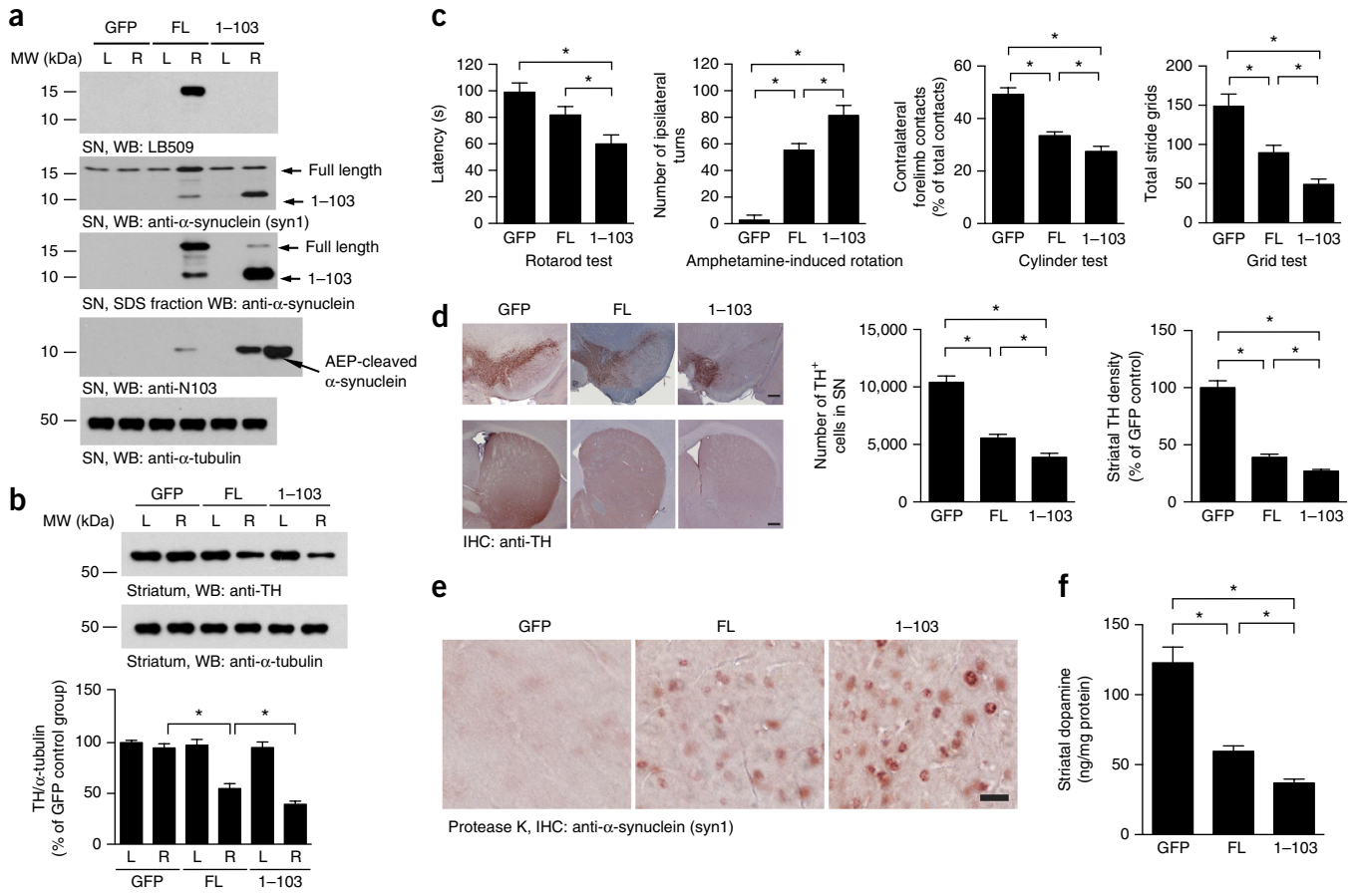


**Figure 5** The α-synuclein$_{1–103}$ fragment induces dopaminergic cell death. (**a**) Western blots (WB) showing the expression of FL α-synuclein and the α-synuclein$_{1–103}$ fragment in SN. α-Tubulin, loading control. L, left; R, right. (**b**) Western blots showing the expression of TH in the striatum, Bar graph, quantification; data are mean ± s.e.m.; $n = 3$ mice; $^*P < 0.05$ by one-way ANOVA. Blots shown are representative of three independent experiments; uncropped images are shown in **Supplementary Data Set 1**. (**c**) The α-synuclein$_{1–103}$ fragment induces behavioral impairment, as demonstrated by rotarod tests, amphetamine-induced rotation tests, cylinder tests and grid tests. Data are mean ± s.e.m.; $n = 9$ mice per group; $^*P < 0.05$ by one-way ANOVA. Source data are available online. (**d**) TH immunostaining of the striatum and SN. Right, unbiased stereological cell counts in the SN and total density of striatal dopaminergic terminals. Scale bars, 200 μm. Bar graph, quantification; data are mean ± s.e.m.; $n = 5$ mice per group; $^*P < 0.05$ by one-way ANOVA. (**e**) Immunostaining showing the aggregation of α-synuclein in SN slides after incubation with 10 μg/ml proteinase K. (**f**) Concentrations of dopamine in the striatal tissues, as determined by HPLC. Data are mean ± s.e.m.; $n = 4$ mice per group; $^*P < 0.05$ by one-way ANOVA. Source data for graphs are available online.

recognizing FL human α-synuclein or the N103 truncation also confirmed these observations (**Fig. 5a**). As expected, overexpression of the α-synuclein$_{1–103}$ fragment resulted in a significant loss of tyrosine hydroxylase (TH) expression in the striatum. In contrast, the effect of FL α-synuclein expression was much less pronounced (**Fig. 5b**). To investigate the effect of the α-synuclein$_{1–103}$ fragment on motor function, we performed a panel of behavioral tests including rotarod tests, amphetamine-induced rotational behavior tests, cylinder tests and grid assays. The rotarod test showed decreased latency in mice injected with AAV-α-synuclein$_{1–103}$ compared with FL α-synuclein (**Fig. 5c**), thus indicating that the α-synuclein$_{1–103}$ fragment triggers much more severe dopaminergic neuronal loss than does FL. In agreement with this finding, overexpression of the α-synuclein$_{1–103}$ fragment, as compared with FL overexpression, produced increased amphetamine-induced rotational asymmetry and increased forepaw impairment (cylinder test) (**Fig. 5c**). The grid test also demonstrated an evident motor deficit in AAV-α-synuclein$_{1–103}$ mice compared with AAV-FL mice (**Fig. 5c**). Together, these behavioral tests indicated that the human α-synuclein$_{1–103}$ fragment induces more severe motor impairment than does the FL counterpart. Quantification of TH immunoreactivity (stereological cell counts of TH-positive neurons and densitometry of TH-positive striatal terminals) supported these findings: the SN and striatum in mice injected with AAV-α-synuclein$_{1–103}$, compared with AAV-α-synuclein FL, contained significantly fewer TH-positive neurons and termini (**Fig. 5d**). Immunostaining of the proteinase K–treated slides indicated more aggregates in mice injected in the SN with AAV-α-synuclein$_{1–103}$ compared with AAV-α-synuclein FL (**Fig. 5e**). Finally, HPLC analysis of striatal tissues showed significantly decreased dopamine concentrations in mice injected with the AAV-α-synuclein$_{1–103}$ fragment compared with AAV-α-synuclein FL (**Fig. 5f**). Hence, these findings demonstrated that the AEP-generated α-synuclein$_{1–103}$ fragment is sufficient to induce a PD-like pattern of neurodegeneration.

### Knockout of AEP ameliorates α-synuclein's pathological effects

We then sought to further confirm the role of AEP in the cleavage of α-synuclein and the subsequent dopaminergic neuronal loss and motor deficits. To do so, we used AAVs to overexpress human α-synuclein in wild-type and AEP-knockout mice. Animals were euthanized 4 months after the injection, and IF analysis confirmed

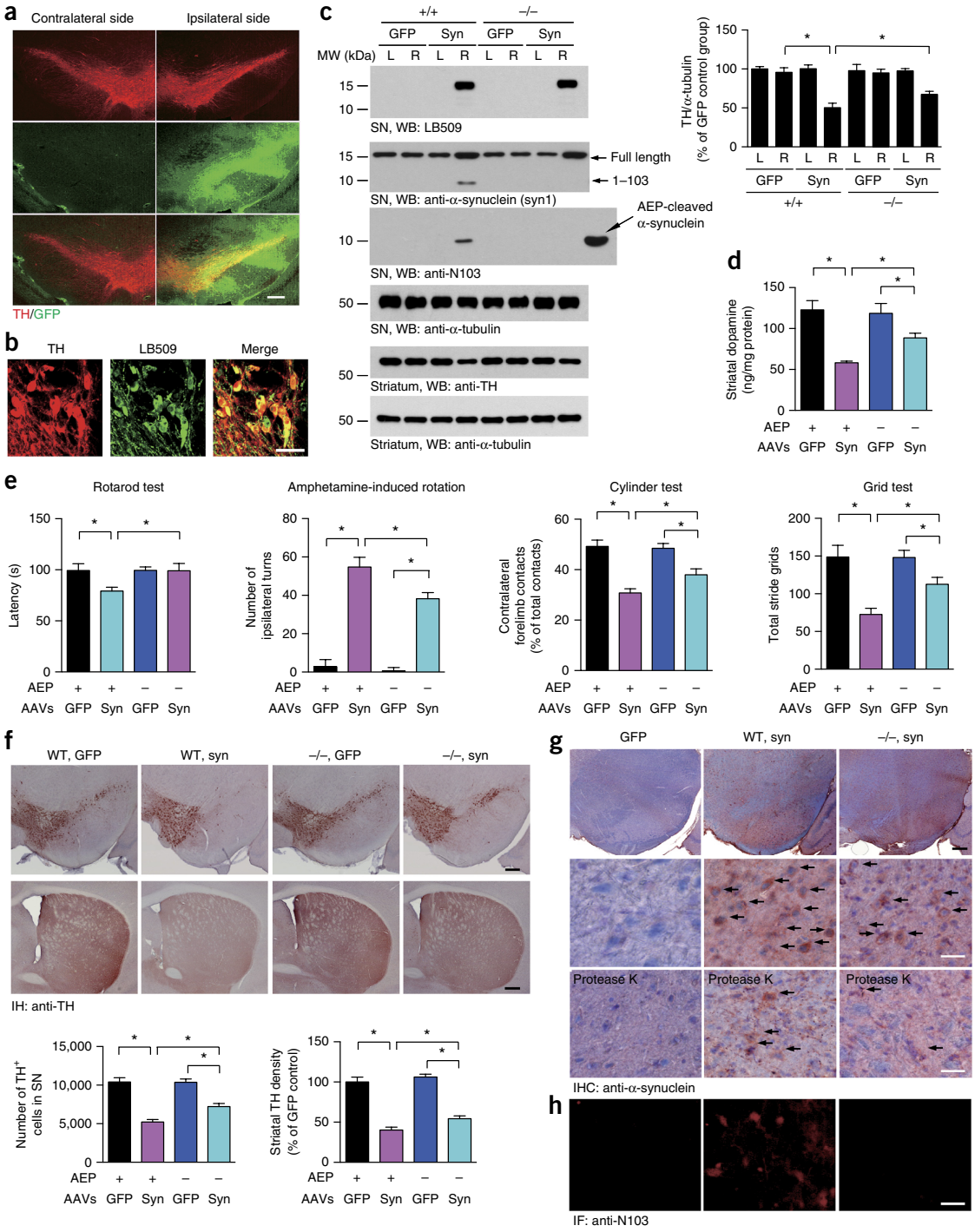


**Figure 6** Deletion of AEP attenuates α-synuclein aggregation and dopaminergic cell death in mice overexpressing human α-synuclein. (**a**) Immunofluorescence showing the expression of AAV-GFP (green) in TH-positive neurons (red). Scale bar, 200 μm. (**b**) Double-label immunofluorescence images showing the AAV-mediated expression of human α-synuclein (green) in TH-positive neurons (red). Scale bar, 50 μm. (**c**) Western blots (WB) showing the expression and truncation of human α-synuclein (syn) in the SN and striatum of wild-type (+/+) and AEP knockout (–/–) mice. L, left; R, right. α-Tubulin, loading control. Bar graph, quantification; data are mean ± s.e.m.; $n = 3$ mice per group; $^*P < 0.05$ by one-way ANOVA. Blots shown are representative of three independent experiments; uncropped images are shown in **Supplementary Data Set 1**. (**d**) Concentrations of dopamine in the striatal tissues, as determined by HPLC. Data are mean ± s.e.m.; $n = 4$ mice per group; $^*P < 0.05$ by one-way ANOVA. (**e**) Effect of AEP deletion on behavioral impairments induced by overexpression of α-synuclein, as shown by rotarod tests, amphetamine-induced rotation tests, cylinder tests and grid tests. Data are mean ± s.e.m.; $n = 9$ AAV-GFP-injected WT mice; $n = 8$ mice in the other three groups; $^*P < 0.05$ by one-way ANOVA. (**f**) TH immunostaining of the striatum and SN. Bottom, unbiased stereological cell counts in the SN and the total density of striatal dopaminergic terminals. Scale bars, 200 μm. Bar graphs, quantification; data are mean ± s.e.m.; $n = 5$; $^*P < 0.05$ by one-way ANOVA. (**g**) α-synuclein aggregation in the SN in AAV-injected mice. The brain slides were stained with anti–human α-synuclein with or without preincubation with proteinase K. The number of proteinase K–resistant α-synuclein inclusions in AEP knockout mice was only half of that in wild-type mice. Black scale bar, 200 μm. White scale bars, 50 μm. (**h**) IHC with anti–α-synuclein N103 antibody, showing the cleavage of α-synuclein in wild-type but not AEP-knockout mice. Scale bar, 50 μm. Source data for graphs are available online.

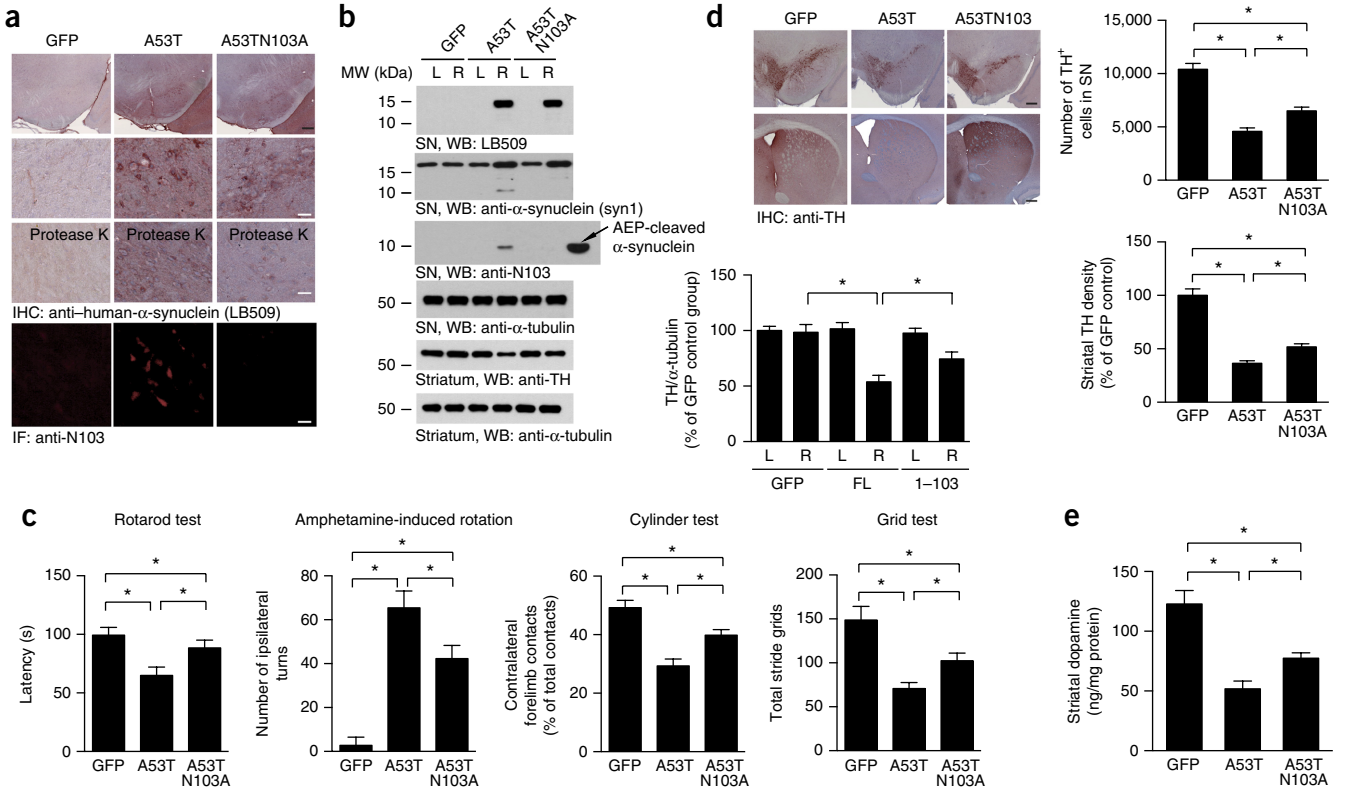


**Figure 7** Preservation of dopaminergic neurons in mice expressing uncleavable α-synuclein A53TN103A. (**a**) Immunostaining of FL α-synuclein and the N103 fragment in the SN in mice. The aggregation of α-synuclein was detected after the slides were preincubated with 10 μg/ml proteinase K. Black scale bar, 200 μm. White scale bars, 50 μm. (**b**) Western blots (WB) showing the expression and truncation of α-synuclein A53T and A53TN103A in the SN and striatum. L, left; R, right. α-Tubulin, loading control. Bar graph, quantification; data are mean ± s.e.m.; $n = 3$; $^*P < 0.05$ by one-way ANOVA. Blots shown are representative of three independent experiments; uncropped images are shown in **Supplementary Data Set 1**. (**c**) The N103A mutation attenuates behavioral impairment induced by α-synuclein A53T. The mice underwent rotarod tests, amphetamine-induced rotation tests, cylinder tests and grid tests. Data are mean ± s.e.m.; $n = 10$ for the A53TN103A group; $n = 9$ for the GFP and A53T groups; $^*P < 0.05$ by one-way ANOVA. (**d**) TH immunostaining of the striatum and SN. Right, unbiased stereological cell counts in the SN and total density of striatal dopaminergic terminals. Data are mean ± s.e.m.; $n = 5$; $^*P < 0.05$ by one-way ANOVA. Scale bar, 200 μm. (**e**) Concentrations of dopamine in the striatal tissues, as determined by HPLC. Data are mean ± s.e.m.; $n = 4$; $^*P < 0.05$ by one-way ANOVA. Source data for graphs are available online.



that TH-positive dopaminergic neurons in the injected SN expressed GFP or human α-synuclein (**Fig. 6a**,**b**). Immunoblotting confirmed these observations. As predicted, FL α-synuclein was selectively cleaved at N103 by AEP in wild-type but not knockout mice. Injection of α-synuclein virus induced a significant striatal TH-immunoreactivity loss. Deletion of AEP partially reversed the loss of striatal TH expression (**Fig. 6c**). Similarly, the striatal dopamine content was significantly decreased in wild-type mice compared with AEP-knockout mice (**Fig. 6d**). In agreement with these observations, overexpression of human α-synuclein induced more severe motor deficits in wild-type mice than GFP control mice, as detected through the motor tests described above. Again, this effect was significantly alleviated in AEP-knockout mice (**Fig. 6e**). A quantitative analysis of TH-positive neurons demonstrated that dopaminergic neurons were drastically lost in the SN, with concomitant denervation of the striatum, when human α-synuclein was overexpressed in wild-type mice, as compared with GFP control mice. This neurotoxic effect was reversed when AEP was depleted (**Fig. 6f**). IHC with anti–human α-synuclein and IF analysis with anti–α-synuclein N103 showed that α-synuclein was successfully overexpressed in the SN regions and that α-synuclein was truncated at N103 in wild-type but not knockout mice (**Fig. 6g**,**h**). The intraneuronal aggregation of α-synuclein was more pronounced in wild-type mice than knockout mice, and the aggregates were partially resistant to proteinase K digestion (**Fig. 6g**). Furthermore, the α-synuclein aggregates exhibited coimmunostaining with 14-3-3 and ubiquitin, thus suggesting that these aggregates were Lewy body–like inclusions (**Supplementary Fig. 7c–f**). Therefore, these data indicated that the deletion of AEP ameliorates α-synuclein fragmentation, attenuates its aggregation and alleviates its neurotoxicity.

### Blockade of α-synuclein (A53T) cleavage by AEP prevents its pathological activities

The A53T mutant of α-synuclein is linked to autosomal-dominant early-onset PD. Transgenic mice expressing mutant A53T show age-dependent formation of intraneuronal α-synuclein inclusions that recapitulate the features in humans with PD, and they also develop severe and complex motor impairment[34,35]. To assess whether these pathological effects caused by the A53T mutant are related to N103 cleavage by AEP, we generated an uncleavable mutant (A53TN103A) that was overexpressed through AAVs in the SN in wild-type mice. Four months after the AAV injection, expression of human α-synuclein (A53T) or its uncleavable mutant was confirmed with IHC. Proteinase K–resistant α-synuclein aggregates were more abundant after expression of A53T as compared with the uncleavable mutant (**Fig. 7a**). IF analysis with anti-N103 antibody showed that A53T proteins were clearly fragmented at N103; in contrast, no cleavage

of A53TN103A proteins was observed (**Fig. 7a**). AEP activity assays indicated that the ratio between cytosolic and lysosomal AEP activities increased in mice injected with AAV-α-synuclein wild type and AAV-α-synuclein A53T, as compared with mice injected with AAV-GFP, thus indicating lysosomal leakage (**Supplementary Fig. 7g**). Immunoblotting verified that both mutants were highly expressed and that the A53T protein was truncated at N103, whereas the uncleavable mutant remained intact. In agreement with our findings above, mice injected with A53TN103A-mutant α-synuclein virus, as compared with A53T mice, were partially spared from motor deficits, thus implicating AEP cleavage of α-synuclein in movement disorders elicited by the A53T mutant (**Fig. 7c**). Accordingly, TH immunoreactivity in both the SN and striatum was significantly lower in A53T-expressing brains than in brains expressing the uncleavable mutant (**Fig. 7b**,**d**). Finally, striatal dopamine concentrations in mice injected with the uncleavable mutant were significantly higher than those in mice injected with the A53T mutant (**Fig. 7e**). Collectively, these data suggested that blockade of α-synuclein (A53T) cleavage by AEP antagonizes its deleterious pathological activities, thus again supporting PD-relevant AEP-mediated truncation of α-synuclein.

## DISCUSSION

AEP is a lysosomal protease that leaks into the cytoplasm in neurodegenerative diseases[26]. Here we report that AEP cleaves human α-synuclein at N103 in an age-dependent manner and triggers α-synuclein aggregation and neurotoxicity, thus leading to dopaminergic neuronal loss and motor impairment. Notably, we found that AEP is highly activated in human PD and LBD brains compared with age-matched healthy controls, especially in the SN. As a consequence, human α-synuclein is cleaved at N103, and this fragment is present in Lewy bodies. In agreement with these observations, we showed that human α-synuclein was cleaved at N103 in human α-synuclein–transgenic mice in an age-dependent manner, and this activity was tightly coupled with the temporal pattern of AEP activity escalation. The age-dependent activation of AEP indicates that AEP expression is gradually increased, and/or endogenous AEP inhibitors, such as cystatin C, are decreased during aging. Furthermore, the pH in the brain gradually decreases during aging[36], and this decrease may elicit AEP activation. Thus, AEP processes α-synuclein in an age-dependent manner. Next, we provided extensive evidence demonstrating that AEP directly cleaves human but not mouse α-synuclein at the N103 residue. Interestingly, although human α-synuclein shares 95% identity with its mouse counterpart, mouse α-synuclein does not have an N103 residue. Notably, the A53T mutation in human α-synuclein causes dominant forms of familial PD, whereas the fifty-third position in wild-type mouse α-synuclein is T (**Supplementary Fig. 2e**). Hence, mouse α-synuclein possesses different key residues from the human version, and these residues may exhibit distinct biological activities.

Cystatin C is the endogenous inhibitor of AEP. Mounting evidence implicates cystatin C in the etiology of neurodegenerative diseases including AD, stroke and epilepsy[37]. During aging, an elevated AEP level and/or decreased cystatin C level may mediate the gradual cleavage of α-synuclein and promote its aggregation during the pathogenesis of synucleinopathies. Here, we also provided evidence that AEP is secreted from lysosomes into the cytoplasm in human PD brains, where it may cleave α-synuclein (**Supplementary Fig. 3**). These observations are consistent with findings from previous reports indicating that the lysosomal AEP penetrates into the cytoplasm in human AD brains and cleaves both tau and SET, a PP2A inhibitor, thereby mediating AD pathogenesis[26]. In fact, AEP has been found to be active in the near-neutral pH milieus of the cytosol, nucleus and cell surface[38].

Post-translational modifications including phosphorylation, truncation and ubiquitination can affect the structure and aggregation properties of α-synuclein[39]. C-terminal truncation promotes α-synuclein fibrillization, in a process mediated by numerous proteases including neurosin, calpain, cathepsin D and metalloproteinase[12]. Nevertheless, the roles of these proteases in the pathogenesis of PD remain elusive. Here we provided extensive biochemical evidence demonstrating that AEP cleaves α-synuclein at N103 in an age-dependent manner. Notably, the cleaved human α-synuclein$_{1–103}$ fragment is more prone to aggregation than the full-length protein (**Fig. 4**) and forms Lewy body-like aggregations in the SN (**Fig. 6**, **Supplementary Fig. 7**), thus providing further evidence of the role of C-terminally truncated α-synuclein in the pathogenesis of neurodegenerative diseases including PD. We observed some minor truncated α-synuclein bands at ~12 kDa in human and mouse brains (**Figs. 1**, **5** and **7**). This result is consistent with previous findings of distinct α-synuclein truncations at sites downstream of N103, including at positions 119 (ref. 14), 121 (ref. 40) and 122 (ref. 18), in synucleinopathies and *in vivo* models. Under different stresses or animal models, a variety of proteases including caspases or calpains may be activated and mediate α-synuclein proteolytic cleavage at various sites, thus contributing to α-synuclein aggregation and neurotoxicity. Nonetheless, AEP cleavage of α-synuclein at N103 during the aging process provides an additional mechanism accounting for AEP's detrimental effect.

To test the hypothesis that AEP cleavage of human α-synuclein contributes to PD pathogenesis, we provided gain-of-function and loss-of-function evidence (**Figs. 5**–**7**). As expected, the human α-synuclein$_{1–103}$ fragment was more potent than FL α-synuclein in provoking dopaminergic neuronal loss and motor deficits (**Fig. 5**). However, although overexpression of FL human α-synuclein in wild-type mice notably produced clear dopaminergic neurodegeneration, as compared with that in GFP controls, far fewer pathological hallmarks were observed in AEP-null mice (**Fig. 6**). This result suggested that AEP promotes the neurotoxic effect of α-synuclein. The same scenario applied to the A53T mutant, which was even more toxic. We demonstrated that blockade of A53T α-synuclein cleavage by AEP greatly suppressed its pathologic activities in PD (**Fig. 7**). Furthermore, the amount of α-synuclein$_{1–103}$ fragments in human PD SN tissue and mouse SN injected with α-synuclein virus was comparable (**Supplementary Fig. 8**), thus suggesting that the amount in the human PD SN was sufficient to induce neurotoxicity. Together, our *in vivo* data support the hypothesis that AEP cleavage of human α-synuclein promotes the onset of PD pathologies. These findings notably indicate that the α-synuclein$_{1–103}$ fragment might act as the major pathological trigger of dopaminergic neuronal loss in PD. Therefore, these findings suggest that AEP may be a novel drug target and that the inhibition of AEP may hold promise as a useful strategy for treating PD.

## METHODS

Methods, including statements of data availability and any associated accession codes and references, are available in the online version of the paper.

*Note: Any Supplementary Information and Source Data files are available in the online version of the paper.*

ACKNOWLEDGMENTS

This work was supported by grants from the Michael J. Fox Foundation (grant ID 11137) to K.Y.; a grant from the National Natural Science Foundation (NSFC) of China (no. 81571249) to Zhentao Zhang; NSFC grant (no. 81528007) to K.Y. and J.-Z.W.; a National Key Basic Research Program of China grant (2010CB945202) to Y.E.S.; an NSFC grant (81330030) to Y.E.S.; and grants from the US Public Health Service (P30EY006360 and R01EY004864) to P.M.I. We thank

the ADRC at Emory University for providing human PD, LBD and healthy-control samples, and C. Watts (University of Cambridge) for providing anti-AEP.

## AUTHOR CONTRIBUTIONS

K.Y. conceived the project, designed the experiments and wrote the manuscript. Zhentao Zhang designed and performed most of the experiments. S.S.K. and X.L. prepared primary neurons and assisted with animal experiments. M.J.B. and F.P.M. provided clones and packaged viral vectors. D.M.D. and N.T.S. performed the mass spectrometry analysis. L.H. and P.M.I. performed the HPLC experiments and critically read and edited the manuscript. Zhaohui Zhang, E.H.A., L.J., Y.E.S., F.P.M. and J.-Z.W. designed the experiments, assisted with data analysis and interpretation and critically read the manuscript.

## COMPETING FINANCIAL INTERESTS

The authors declare no competing financial interests.




1. Maries, E., Dass, B., Collier, T.J., Kordower, J.H. & Steece-Collier, K. The role of alpha-synuclein in Parkinson's disease: insights from animal models. *Nat. Rev. Neurosci.* **4**, 727–738 (2003).
2. Polymeropoulos, M.H. *et al.* Mutation in the alpha-synuclein gene identified in families with Parkinson's disease. *Science* **276**, 2045–2047 (1997).
3. Krüger, R. *et al.* Ala30Pro mutation in the gene encoding α-synuclein in Parkinson's disease. *Nat. Genet.* **18**, 106–108 (1998).
4. Leroy, E., Boyer, R. & Polymeropoulos, M.H. Intron-exon structure of ubiquitin c-terminal hydrolase-L1. *DNA Res.* **5**, 397–400 (1998).
5. Kitada, T. *et al.* Mutations in the parkin gene cause autosomal recessive juvenile parkinsonism. *Nature* **392**, 605–608 (1998).
6. Spillantini, M.G. *et al.* α-Synuclein in Lewy bodies. *Nature* **388**, 839–840 (1997).
7. Olanow, C.W. & Brundin, P. Parkinson's disease and alpha synuclein: is Parkinson's disease a prion-like disorder? *Mov. Disord.* **28**, 31–40 (2013).
8. Masliah, E. *et al.* Dopaminergic loss and inclusion body formation in alpha-synuclein mice: implications for neurodegenerative disorders. *Science* **287**, 1265–1269 (2000).
9. Kahle, P.J., Neumann, M., Ozmen, L. & Haass, C. Physiology and pathophysiology of alpha-synuclein: cell culture and transgenic animal models based on a Parkinson's disease-associated protein. *Ann. NY Acad. Sci.* **920**, 33–41 (2000).
10. Feany, M.B. & Bender, W.W.A. *Drosophila* model of Parkinson's disease. *Nature* **404**, 394–398 (2000).
11. Burré, J. *et al.* Properties of native brain α-synuclein. *Nature* **498**, E4–E6 (2013).
12. Lashuel, H.A., Overk, C.R., Oueslati, A. & Masliah, E. The many faces of α-synuclein: from structure and toxicity to therapeutic target. *Nat. Rev. Neurosci.* **14**, 38–48 (2013).
13. Li, W. *et al.* Aggregation promoting C-terminal truncation of alpha-synuclein is a normal cellular process and is enhanced by the familial Parkinson's disease-linked mutations. *Proc. Natl. Acad. Sci. USA* **102**, 2162–2167 (2005).
14. Liu, C.W. *et al.* A precipitating role for truncated alpha-synuclein and the proteasome in alpha-synuclein aggregation: implications for pathogenesis of Parkinson disease. *J. Biol. Chem.* **280**, 22670–22678 (2005).
15. Hoyer, W., Cherny, D., Subramaniam, V. & Jovin, T.M. Impact of the acidic C-terminal region comprising amino acids 109-140 on alpha-synuclein aggregation in vitro. *Biochemistry* **43**, 16233–16242 (2004).
16. Murray, I.V. *et al.* Role of alpha-synuclein carboxy-terminus on fibril formation *in vitro*. *Biochemistry* **42**, 8530–8540 (2003).
17. Mishizen-Eberz, A.J. *et al.* Distinct cleavage patterns of normal and pathologic forms of alpha-synuclein by calpain I *in vitro*. *J. Neurochem.* **86**, 836–847 (2003).
18. Mishizen-Eberz, A.J. *et al.* Cleavage of alpha-synuclein by calpain: potential role in degradation of fibrillized and nitrated species of alpha-synuclein. *Biochemistry* **44**, 7818–7829 (2005).
19. Sevlever, D., Jiang, P. & Yen, S.H. Cathepsin D is the main lysosomal enzyme involved in the degradation of alpha-synuclein and generation of its carboxy-terminally truncated species. *Biochemistry* **47**, 9678–9687 (2008).
20. Takahashi, M. *et al.* Oxidative stress-induced phosphorylation, degradation and aggregation of alpha-synuclein are linked to upregulated CK2 and cathepsin D. *Eur. J. Neurosci.* **26**, 863–874 (2007).
21. Halfon, S., Patel, S., Vega, F., Zurawski, S. & Zurawski, G. Autocatalytic activation of human legumain at aspartic acid residues. *FEBS Lett.* **438**, 114–118 (1998).
22. Gamblin, T.C. *et al.* Caspase cleavage of tau: linking amyloid and neurofibrillary tangles in Alzheimer's disease. *Proc. Natl. Acad. Sci. USA* **100**, 10032–10037 (2003).
23. Alvarez-Fernandez, M. *et al.* Inhibition of mammalian legumain by some cystatins is due to a novel second reactive site. *J. Biol. Chem.* **274**, 19195–19203 (1999).
24. Liu, Z. *et al.* Neuroprotective actions of PIKE-L by inhibition of SET proteolytic degradation by asparagine endopeptidase. *Mol. Cell* **29**, 665–678 (2008).
25. Madeira, A., Pommet, J.M., Prochiantz, A. & Allinquant, B. SET protein (TAF1beta, I2PP2A) is involved in neuronal apoptosis induced by an amyloid precursor protein cytoplasmic subdomain. *FASEB J.* **19**, 1905–1907 (2005).
26. Basurto-Islas, G., Grundke-Iqbal, I., Tung, Y.C., Liu, F. & Iqbal, K. Activation of asparaginyl endopeptidase leads to Tau hyperphosphorylation in Alzheimer disease. *J. Biol. Chem.* **288**, 17495–17507 (2013).
27. Herskowitz, J.H. *et al.* Asparaginyl endopeptidase cleaves TDP-43 in brain. *Proteomics* **12**, 2455–2463 (2012).
28. Zhang, Z. *et al.* Cleavage of tau by asparagine endopeptidase mediates the neurofibrillary pathology in Alzheimer's disease. *Nat. Med.* **20**, 1254–1262 (2014).
29. Zhang, Z. *et al.* Delta-secretase cleaves amyloid precursor protein and regulates the pathogenesis in Alzheimer's disease. *Nat. Commun.* **6**, 8762 (2015).
30. Li, D.N., Matthews, S.P., Antoniou, A.N., Mazzeo, D. & Watts, C. Multistep autoactivation of asparaginyl endopeptidase *in vitro* and *in vivo*. *J. Biol. Chem.* **278**, 38980–38990 (2003).
31. Chen, L. *et al.* Tyrosine and serine phosphorylation of alpha-synuclein have opposing effects on neurotoxicity and soluble oligomer formation. *J. Clin. Invest.* **119**, 3257–3265 (2009).
32. Ellis, C.E., Schwartzberg, P.L., Grider, T.L., Fink, D.W. & Nussbaum, R.L. α-Synuclein is phosphorylated by members of the Src family of protein-tyrosine kinases. *J. Biol. Chem.* **276**, 3879–3884 (2001).
33. Beyer, K. & Ariza, A. α-Synuclein posttranslational modification and alternative splicing as a trigger for neurodegeneration. *Mol. Neurobiol.* **47**, 509–524 (2013).
34. Giasson, B.I. *et al.* Neuronal alpha-synucleinopathy with severe movement disorder in mice expressing A53T human alpha-synuclein. *Neuron* **34**, 521–533 (2002).
35. Lee, M.K. *et al.* Human alpha-synuclein-harboring familial Parkinson's disease-linked Ala-53 → Thr mutation causes neurodegenerative disease with alpha-synuclein aggregation in transgenic mice. *Proc. Natl. Acad. Sci. USA* **99**, 8968–8973 (2002).
36. Forester, B.P. *et al.* Age-related changes in brain energetics and phospholipid metabolism. *NMR Biomed.* **23**, 242–250 (2010).
37. Gauthier, S., Kaur, G., Mi, W., Tizon, B. & Levy, E. Protective mechanisms by cystatin C in neurodegenerative diseases. *Front. Biosci. (Schol. Ed.)* **3**, 541–554 (2011).
38. Dall, E. & Brandstetter, H. Structure and function of legumain in health and disease. *Biochimie* **122**, 126–150 (2016).
39. Oueslati, A., Fournier, M. & Lashuel, H.A. Role of post-translational modifications in modulating the structure, function and toxicity of alpha-synuclein: implications for Parkinson's disease pathogenesis and therapies. *Prog. Brain Res.* **183**, 115–145 (2010).
40. Wang, W. *et al.* Caspase-1 causes truncation and aggregation of the Parkinson's disease-associated protein α-synuclein. *Proc. Natl. Acad. Sci. USA* **113**, 9587–9592 (2016).

## ONLINE METHODS

**Mice.** Human *SNCA*–transgenic mice carrying a transgene containing the human *SNCA* gene and a knockout allele of the mouse *Snca* gene were from Jackson Laboratory (stock no. 023837). The AEP-knockout mice on a mixed 129/Ola and C57BL/6 background were generated as previously reported[41]. Only male mice were used in the experiments. Animal care and handling was performed according to Emory Medical School guidelines. Sample size was determined in Power and Precision software (Biostat). The mice were randomized into different groups by using a random number table. Investigators were blinded to the group allocation during the animal experiments. The protocol was reviewed and approved by the Emory Institutional Animal Care and Use Committee.

**Human tissue samples.** Postmortem brain samples were dissected from the frozen brains of five control cases, LBD cases, and PD cases obtained from the Emory Alzheimer's Disease Research Center. The study was approved by the biospecimen committee at Emory University. PD and LBD cases were clinically diagnosed and neuropathologically confirmed. Informed consent was obtained from all subjects.

**Cell lines, transfection and infection.** HEK293 cells were obtained from the ATCC and tested for mycoplasma contamination before use. Cells were transfected with plasmids encoding wild-type or point-mutant GFP-α-synuclein, myc-AEP, myc–AEP C189S, or myc–AEP N323A by the calcium phosphate precipitation method. AAVs were used to express wild-type, mutant and truncated α-synuclein in primary neurons and SH-SY5Y cells. The neurotoxicity was analyzed through TUNEL analysis or LDH assays.

***In vitro* α-synuclein cleavage assay.** To assess the cleavage of α-synuclein by AEP *in vitro*, HEK293 cells were transfected with GST- or GFP-tagged α-synuclein DNA through the calcium phosphate precipitation method. 48 h after transfection, cells were collected, washed once in PBS, lysed in buffer (50 mM sodium citrate, 5 mM DTT, 0.1% CHAPS, pH 5.5, and 0.5% Triton X-100), and centrifuged for 10 min at 14,000*g* at 4 °C. The supernatant was then incubated with mouse kidney lysate or recombinant AEP at pH 7.4 or 6.0 at 37 °C for different time points. To test the effects of cathepsin, calpain and AEP inhibitors on the cleavage of α-synuclein by AEP, inhibitors were used against cathepsin (E64, Sigma-Aldrich), calpains (ALLN, Sigma-Aldrich) and AEP (AENK peptide inhibitor and inactive control AEQK). To measure the cleavage of purified α-synuclein fragments by AEP, GST-tagged α-synuclein was purified with glutathione beads. The purified α-synuclein protein was incubated with recombinant AEP protein (Novoprotein, 5 μg $ml^{-1}$) in buffer (50 mM sodium citrate, 5 mM DTT, 0.1% CHAPS and 0.5% Triton X-100, pH 6.0). The samples were then boiled in 1× SDS loading buffer and analyzed by immunoblotting.

**AEP activity assay.** Tissue homogenates or cell lysates (10 μg) were incubated in 200 μl assay buffer (20 mM citric acid, 60 mM $Na_2HPO_4$, 1 mM EDTA, 0.1% CHAPS and 1 mM DTT, pH 6.0) containing 20 μM AEP substrate Z-Ala-Ala-Asn-AMC (Bachem). AMC released by substrate cleavage was quantified by measuring at 460 nm in a fluorescence plate reader at 37 °C for 1 h in kinetic mode for 5 min.

**Mass spectrometry analysis.** Protein samples were in-gel-digested with 10 ng/μl Glu-C. Peptide samples were resuspended in loading buffer (0.1% formic acid, 0.03% trifluoroacetic acid and 1% acetonitrile) and loaded onto a 20-cm nano-HPLC column (internal diameter, 75 μm) packed with Reprosil-Pur 120 C18-AQ 1.9-μm beads (Dr. Maisch) and eluted over a 2-h 1–50% buffer B reverse-phase gradient (buffer A, 0.1% formic acid and 1% acetonitrile in water; buffer B, 0.1% formic acid in acetonitrile) generated by a Dionex RSLCnano UPLC system (Thermo). Peptides were ionized with 2.0-kV electrospray ionization voltage from a nano-ESI source on an Orbitrap Fusion mass spectrometer (Thermo). Data-dependent acquisition of MS spectra at 120,000 resolution (FWHM), and MS/MS spectra were obtained in the Orbitrap after electron-transfer dissociation (ETD) with supplemental activation with high energy (EThcD) for peptide masses corresponding to the 3+ and 4+ charge states (645.3536 and 484.2669, respectively) of the peptide GAGSIAAATGFVKKDQLGKN. To identify AEP-cleavage sites in human α-synuclein, Proteome Discoverer 2.0 (PD) was used to search and match MS/MS spectra to a complete human proteome database (NCBI reference sequence revision 62, with 68746 entries) with a ±10-p.p.m. mass-accuracy threshold and allowable cleavages at glutamates and asparagines. A percolator was used to filter the peptide spectral matches (PSM) to a false discovery rate (FDR) of <1%. All MS/MS spectra for putative AEP-generated α-synuclein cleavage sites were manually inspected.

**Generation of antibodies specific to AEP-generated α-synuclein (anti–α-synuclein N103).** Two rabbits were immunized with the peptide Ac-CVKKDQLGKN-OH, which included the nine amino acids in α-synuclein that precede the AEP-cleavage site at N103 as well as an N-terminal cysteine residue to allow for coupling to KLH. The rabbits were received booster injections four times with the immunizing peptide with 3-week intervals between injections. The antiserum was affinity purified by chromatography with the immunizing peptide and was then absorbed to a spanning peptide spanning the N103 cleavage site (Ac-CKDQLGKNEEGAPQE-amide). The titers against the immunizing peptide were determined by ELISA. The maximal dilution giving a positive response with chromogenic substrate for horseradish peroxidase was 1:30,000. The immunoactivity of the antiserum was further confirmed by western blotting and immunohistochemistry.

**Western blot analysis.** The mouse brain tissue or human tissue samples were lysed in lysis buffer (50 mM Tris, pH 7.4, 40 mM NaCl, 1 mM EDTA, 0.5% Triton X-100, 1.5 mM $Na_3VO_4$, 50 mM NaF, 10 mM sodium pyrophosphate and 10 mM sodium β-glycerophosphate, supplemented with a cocktail of protease inhibitors), and centrifuged for 15 min at 16,000*g*. The supernatant was boiled in SDS loading buffer. After SDS–PAGE, the samples were transferred to a nitrocellulose membrane. Primary antibodies to the following targets were used: GST-HRP (Sigma-Aldrich, GERPN1236), α-tubulin (Sigma-Aldrich, T9026), HA (Santa Cruz, H3663), myc (Santa Cruz, M4439), α-synuclein N terminus (Santa Cruz, sc-514908); anti-α-synuclein (syn1, clone 42, BD Bioscience, 610787), AEP (clone 6E3, gift from C. Watts), TH (Cell Signaling Technology, 2792), α-synuclein C terminus (Cell Signaling Technology, 2642) and α-synuclein LB509 (Thermo Fisher Scientific, 180215).

**Immunostaining.** Paraffin-embedded human brain sections or free-floating mouse brain sections were treated with 0.3% $H_2O_2$ for 10 min. Sections were thereafter washed three times in PBS, blocked in 1% BSA and 0.3% Triton X-100 for 30 min and incubated overnight with anti-TH (1:1,000) antibody, anti–α-synuclein N103 antibody (1:1,000) or α-synuclein LB509 antibody (1:500) at 4 °C. The signal was developed with a Histostain-SP kit (Invitrogen). To detect the localization of the α-$synuclein_{1–103}$ fragment in Lewy bodies in human PD brain sections, the sections were incubated with rabbit anti–α-synuclein N103 primary antibody and mouse anti-α-synuclein antibody overnight at 4 °C. The slides were washed three times in PBS and incubated with Texas red–conjugated anti-mouse IgG and FITC-conjugated anti-rabbit IgG for 1 h at room temperature. The slides were washed three times in PBS, then covered with a glass cover with mounting solution and examined under a fluorescence microscope (Olympus). The primary cultured neurons were infected with AAVs encoding full-length α-synuclein or the α-$synuclein_{1–103}$ fragment, and were double-stained for α-synuclein/TH, TUNEL/TH or TH/N103. The percentages of $TUNEL^+/TH^+$ cells over $TH^+$ cells were calculated. The researchers who performed immunostaining and cell counting were blinded to the group allocations.

**Coimmunoprecipitation.** The mouse brain tissue samples were lysed in lysis buffer (50 mM Tris, pH 7.4, 40 mM NaCl, 1 mM EDTA, 0.5% Triton X-100, 1.5 mM $Na_3VO_4$, 50 mM NaF, 10 mM sodium pyrophosphate and 10 mM sodium β-glycerophosphate, supplemented with a cocktail of protease inhibitors) and centrifuged for 15 min at 16,000*g*. The supernatant was incubated with anti-α-synuclein antibody and Protein A/G–agarose overnight at 4 °C. After extensive washing with lysis buffer, the bound proteins were eluted from the beads by boiling in Laemmli sample buffer and were subjected to western blot analyses.

***In vitro* aggregation of α-synuclein.** The aggregation of α-synuclein was induced as described previously[42]. Briefly, purified α-synuclein protein (rPeptide, 5 mg $ml^{-1}$) was first incubated with vehicle or AEP in for 1 h and then dialyzed against PBS, pH 7.0. The samples were incubated at 37 °C with continuous shaking for 3 d. The aggregation kinetics of α-synuclein was measured with thioflavin T staining. 100 μl of 20 μM thioflavin T was mixed with 2 μl α-synuclein protein




doi:10.1038/nsmb.3433

and incubated for 5–10 min at room temperature. Fluorometric readings were taken at 450-nm excitation and 510-nm emission. The remaining solutions of aggregated α-synuclein were centrifuged at 100,000*g* for 30 min to separate the aggregated α-synuclein pellet and the nonaggregated α-synuclein supernatant, and analyzed by western blotting.

**AAV vector packaging and stereotaxic injection.** 293T cells were transfected with a plasmid encoding the viral genome together with a plasmid encoding AAV2 rep, AAV5 cap, as well as helper functions. 72 h post-transduction, virus particles were harvested by repeated freeze–thaw cycles, purified with an iodixanol gradient and subsequent column chromatography, dialyzed against modified (enhanced $Mg^{2+}/Ca^{2+}$) PBS and concentrated to the desired titer with an Apollo concentrator (Orbital Biosciences). Three-month-old wild-type C57BL/6J mice were anesthetized with phenobarbital (75 mg $kg^{-1}$). Unilateral intracerebral injection of AAVs was performed stereotaxically at coordinates anteroposterior (AP) −3.1 mm and mediolateral (ML) −1.2 mm relative to the bregma, and dorsoventral (DV) −4.0 mm from the dural surface. 2 µl of viral suspension containing $3 \times 10^{13}$ vector genomes (vg) $ml^{-1}$ was injected into each site with a 10-µl glass syringe with a fixed needle at a rate of 0.25 µl $min^{-1}$. The needle remained in place for 5 min before it was removed slowly (over 2 min). The mice were placed on a heating pad until they began to recover from the surgery.

**Primary neuron cultures.** Primary rat ventral midbrain culture neurons were cultured as previously described[43]. To measure the effects of α-synuclein fragments on neurons, neurons cultured 7 d *in vitro* (DIV 7) were infected with AAVs encoding FL α-synuclein or α-synuclein$_{1-103}$. 5 d later, the neurons were fixed in 4% formaldehyde, permeabilized and immunostained with anti-TH antibody. The toxic effect of α-synuclein fragments was detected with an *In situ* cell death detection kit (Roche). The apoptotic index was expressed as a percentage of TUNEL-positive neurons out of the total number of TH-positive neurons.

**Behavioral tests.** Motor impairments were tested 15 weeks after the virus injection with rotarod tests, cylinder tests, amphetamine-induced rotation tests, and grid tests. In the rotarod tests, animals were trained for 2 min at a speed of 4 r.p.m. After this initial training, mice performed eight trials for a maximum of 5 min with increasing speed starting from 4 r.p.m. and increasing to 40 r.p.m. The fall-off time was recorded. In the cylinder tests, mice were placed individually inside a glass cylinder (12-cm diameter, 22 cm-height). Video recordings were examined by an observer blinded to the animal's identity. Between 20 and 30 wall touches per animal (contacts with fully extended digits executed with the forelimb ipsilateral and contralateral to the lesion) were counted. In the amphetamine-induced rotation tests, animals that had been unilaterally injected with AAV vectors were challenged with D-amphetamine (free base, 2 mg/kg in saline, intramuscular, Sigma). The number of completed circles either to the left or to the right was counted.

**Stereological quantification of TH-positive cells.** The number of TH-positive cells in the SN was estimated with a random-sampling stereological counting method. For each animal, every fourth section throughout the rostrocaudal extent of the SN and every fourth section covering the entire extent of the STR were incorporated into the counting procedure. The investigator was blinded to the conditions of the experiment.

**HPLC analysis of dopamine.** Dopamine levels were determined by HPLC with coulometric detection through established methods[44]. Each brain sample was processed individually. Samples were homogenized in 0.1 N $HClO_4$ solution (containing 0.01% sodium metabisulfite and 25 ng/ml internal standard 3, 4-dihydroxybenzylamine HBr) and centrifuged at 13,000*g* for 15 min at 4 °C. Aliquots of supernatant fractions were filtered with a 0.2-µm HT Tuffryn membrane (Pall), then injected into an Ultrasphere 5 µm ODS column, 250 × 4.6-mm (Hichrom Limited) and separated with a mobile phase containing 0.1 M sodium phosphate, 0.1 mM EDTA, 0.30 mM sodium octyl sulfate and 5% (v/v) acetonitrile, pH 3.2. The dopamine amount (ng/sample) was then quantified by comparison to internal standards, with a standard curve generated with 0.1–5 ng of dopamine standard. The protein level (mg/sample) was determined with Lowry protein assays with a standard curve generated with 0–95 µg bovine serum albumin[45].

**Statistical analysis.** Statistical analysis was performed with either Student's *t* test (two-group comparison) or one-way ANOVA followed by LSD *post hoc* test (more than two groups), and differences with $P$ values <0.05 were considered significant. Detailed information on the experimental design and reagents can be found in the **Life Sciences Reporting Summary**.

**Data availability.** Source data files for **Figures 1–7** are available online. All other data are available from the corresponding author upon reasonable request.


41. Shirahama-Noda, K. *et al.* Biosynthetic processing of cathepsins and lysosomal degradation are abolished in asparaginyl endopeptidase-deficient mice. *J. Biol. Chem.* **278**, 33194–33199 (2003).
42. Volpicelli-Daley, L.A., Luk, K.C. & Lee, V.M. Addition of exogenous α-synuclein preformed fibrils to primary neuronal cultures to seed recruitment of endogenous α-synuclein to Lewy body and Lewy neurite-like aggregates. *Nat. Protoc.* **9**, 2135–2146 (2014).
43. Zhang, Z. *et al.* 7,8-dihydroxyflavone prevents synaptic loss and memory deficits in a mouse model of Alzheimer's disease. *Neuropsychopharmacology* **39**, 638–650 (2014).
44. Pozdeyev, N. *et al.* Dopamine modulates diurnal and circadian rhythms of protein phosphorylation in photoreceptor cells of mouse retina. *Eur. J. Neurosci.* **27**, 2691–2700 (2008).
45. Lowry, O.H., Rosebrough, N.J., Farr, A.L. & Randall, R.J. Protein measurement with the Folin phenol reagent. *J. Biol. Chem.* **193**, 265–275 (1951).